Korean Journal of Environmental Biology

Spatial distribution of phytoplankton in Gamak Bay in spring, with emphasis on small phytoplankton

Yeongji Oh and Yoonja Kang*

Department of Ocean Integrated Science, Chonnam National University, Yeosu 56828, Republic of Korea

*Corresponding author
Yoonja Kang
Tel. 061-659-7141
E-mail. yoonjakang@jnu.ac.kr

Abstract: Phytoplankton communities, with emphasis on picoplankton and nanoplankton, were investigated in Gamak Bay, South Korea, where freshwater input and coastal water intrusion shape ecosystem functions. Shellfish farms and fish farms are located in the inner bay and outer bay, respectively, and tides translocate uneaten food and urine production from aquaculture farms toward the inner bay. Water masses were distinctly different based on a significantly different density between the surface and bottom layer and among three water masses, including the inner bay, outer bay, and Yeosu Harbor. Phytoplankton communities were quantified using flow cytometry and size-fractionated chlorophyll-a (chl-a) was measured. Salinity was a principal variable separating phytoplankton communities between the surface and bottom layer, whereas $Si(OH)_4$ controlled the communities in the inner bay, and NH_4^+ and PO_4^{3-} governed the outer bay communities. While phycocyanin-containing (PC) cyanobacteria dominated in the outer bay, phycoerythrin-containing (PE) cyanobacteria dominance occurred with cryptophyte dominance, indicating that nutrients affected the distribution of pico- and nanoplankton and that cryptophytes potentially relied on a mixotrophic mode by feeding on PE cyanobacteria. Interestingly, picoeukaryotes and eukaryotes larger than 10 μm were mostly responsible for the ecological niche in the western region of the bay. Given that chl-a levels have historically declined, our study highlights the potential importance of increased small phytoplankton in Gamak Bay. Particularly, we urge an examination of the ecological role of small phytoplankton in the food supply of cultivated marine organisms.

Keywords: picoplankton, nanoplankton, small phytoplankton, coastal waters, aquacultures

INTRODUCTION

Phytoplankton are responsible for more than 50% of primary production in coastal waters across the globe as they trigger the biogeochemical cycles and transfer carbon energy through marine food webs (Cloern *et al.* 2014). Particularly, anthropogenic activity-driven nutrient loadings (Paerl *et al.* 2014) and excessive nutrient input from aquaculture farms (Bouwman *et al.* 2013b) cause eutrophication, thereby governing phytoplankton biomass and species composition in communities. The eutrophication often results in harmful algal blooms, which disrupt ecosystem functions in coastal waters (Glibert *et al.* 2018). While during this century eutrophication driven by human activities has been a central problem in coastal ecosystems (Sinha *et al.* 2017), an amount of nutrients originating from aquaculture farms is substantial (Bouwman *et al.* 2013b) and the extent which the nutrients exacerbate coastal ecosystems will increase six

times by 2050 (Bouwman *et al.* 2013a).

Dominance of small phytoplankton such as picoplankton and nanoplankton often occur in the estuarine ecosystems because of reduced river discharge and relatively more effects of sewage treatment plants (Kim *et al.* 2019; Kang *et al.* 2020). Although picoplankton actively proliferate in oligotrophic and high temperature environment, where they can be superior to microplankton (Raven 1998; Agawin *et al.* 2000), a variety of picoplankton including autotrophic cyanobacteria and picoeukaryotes also comprise of major phytoplankton communities in coastal waters (Worden *et al.* 2004; Wu *et al.* 2014; Kang *et al.* 2015; Kang and Oh 2021). In Gamak Bay located in Yeosu Channel, which connects Gwangyang Bay and the South Sea, freshwater flowing into the bay through the northwestern channel and nutrient loadings from Seomjin River and Yeondeung Creek substantially contribute to nutrient components. In addition, shellfish farms in the northern part of the bay, oyster farms in the central part of the bay, and fish farms in the southern channel of the bay are another major point sources of nutrients (Lee *et al.* 2020). Given that prevailing of various aquaculture farms throughout the bay, nutrient input from adjacent aquaculture farms may not be negligible.

Multiple studies of the spatial and temporal phytoplankton distribution have been investigated in Gamak Bay for the last decade. Phytoplankton communities were identified using high performance liquid chromatography with CHEMTAX analysis (Oh *et al.* 2008a) and the phytoplankton distribution was described with environmental variations (Yoon 2000; Oh *et al.* 2009). Kwon *et al.* (2011) revealed that the activity of alkaline phosphatase and alkaline phosphatase-hydrolysable phosphorus is of importance for phytoplankton to acquire an ecological niche. Studies of phytoplankton ecology in Gamak Bay have mostly focused on microplankton such as diatoms or dinoflagellates that are observable with microscopy but no studies of picoplankton or nanoplankton ecology have been performed. Conventionally, picoplankton are abundant in the open sea relying on regenerated nutrients and microplankton dominate in eutrophic coastal waters (Cloern 2018). Recently, coastal waters have shifted towards environments where picoplankton and nanoplankton can be favored (Ansotegui *et al.* 2003; Kang *et al.* 2019, 2020).

Thus, we first investigated the spatial distribution of size-fractionated phytoplankton (picoplankton, nanoplankton, and microplankton) with physical-chemical variables in Gamak Bay, to enlighten the importance of small phytoplankton in the coastal ecosystems, particularly adjacent to aquaculture farms. Size-fractionated chlorophyll-a (chl-a) and phytoplankton groups quantified using flow cytometry were focused using the multivariate analyses.

MATERIALS AND METHODS

1. Study region

Gamak Bay is located around the archipelago off southwestern Korea, and is a semi-enclosed bay connecting between Yeosu Hwayang-myeon and Dolsan-eup with a length of 15 km and area of 112 km^2 (Fig. 1). We investigated five stations, where the Korea Marine Environment Management Corporation (KOEM) have seasonally and regularly monitored for a decade to evaluate the marine ecology and environmental conditions, and the National Institute of Fisheries Science (NIFS) has monitored to estimate water quality associated with the dominant aquaculture farms. Three distinct water masses included the northern inner bay water (here after, the inner bay), Yeosu harbor water in the northern narrow channel influenced by Seomjin River and Yeondung Creek (Yeosu harbor), and the southern outer bay water (the outer bay) (Lee and Cho 1990). During flood tide, a substantial amount of seawater intrudes through the southern channel of the bay and during ebb tide, the bay waters escape via the northeastern channel and the southern channel (Kim *et al.* 2012). Exogenous matter and tides affect the three water masses (i.e., inner bay, Yeosu harbor, and outer bay) while the northern region in the bay experiences eutrophication due to considerable accumulation of organic matter (Yoon 2000). In addition, in the northern region of Gamak Bay, hypoxic water masses frequently occur in summer (Lee and Cho 1990; Lee 1992; Kim *et al.* 2006, 2010; Kim *et al.* 2011). These characteristics of the northern waters can affect the center of the bay.

2. Field survey

Samples were collected at five stations on May 28–29, 2021 during a cruise with R/V Cheongkyung using a Niskin water sampler (General Oceanics, Miami, FL, USA) from the surface and bottom layers at 1 m below the water surface and 1 m above the surface sediments, respectively (Fig. 1). Samples for chl-a, flow cytometry, and dissolved inorganic nitrogen (NO_3^-, NO_2^-, NH_4^+, PO_4^{3-}, and $Si(OH)_4$) were generated on board. Temperature, salinity, dissolved oxygen (DO), and pH were measured on the surface water using
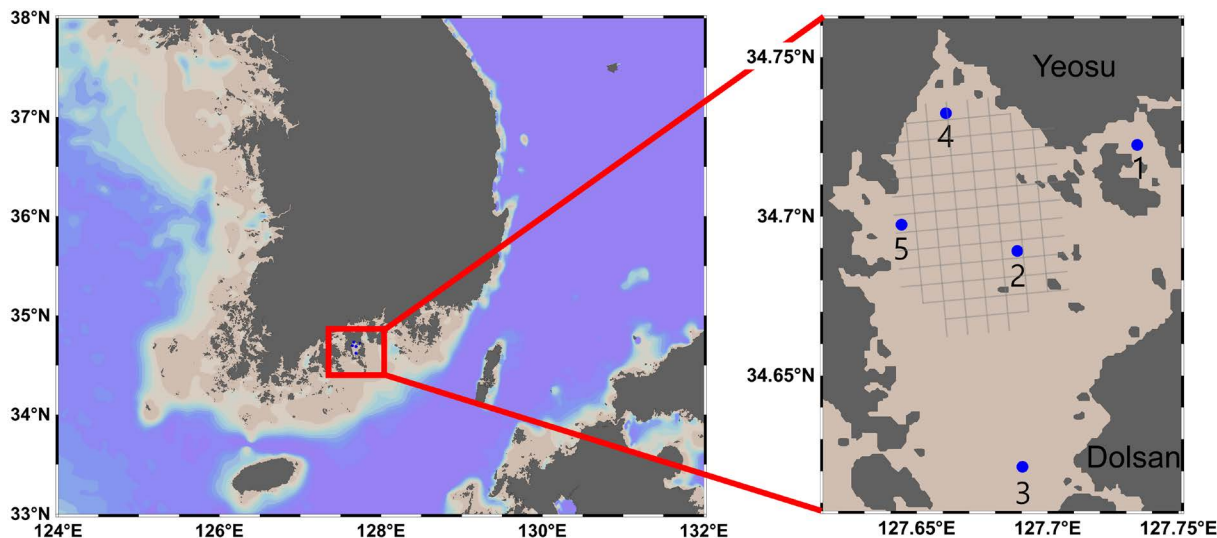
Fig. 1. Map showing sampling stations in Gamak Bay in the southern coastal waters of Korea. The crosshatch pattern and diagonal hatch pattern indicate long-lined oyster and mussel farms and fish cages, respectively.

YSI ProDSS (YSI Inc., Yellow Springs, OH, USA) while the physical variables of the bottom water were obtained from the Marine Environment Information System (www. meis.go.kr) due to lack of data. Transparency was measured using a secchi disk. For total chl-a, the collected seawater was filtered onto GF/F (47 mm in diameter; Whatman plc, Maidstone, UK) and the size-fractionated chl-a samples were generated by sequentially filtering onto polycarbonate filters with different pore sizes (20 μm polycarbonate track etched membrane filter 47 mm diameter, GVS North America, ME, USA; 10 μm polycarbonate membrane filter Isopore plc; GF/F filter Whatman plc, Maidstone, UK). Because picoplankton with a size of 3 μm or larger were often observed (Kang *et al.* 2015), 10 μm filters was used to define small phytoplankton including pico- and nanoplankton. Flow cytometric samples were prepared by adding 0.5 mL of 10% buffered formalin into 4.5 mL of seawater and storing at $-80°C$ until analysis. Adding 1−2% final concentration buffered formalin considers the most optimal preservation method for phytoplankton community analysis when flow cytometry is applied (Poulton and Martin 2010). 20 mL of seawater were filtered onto pre-combusted GF/F filters (25 mm, 450°C for 2 h) to produce dissolved inorganic nitrogen samples and were stored at $-80°C$ until analysis.

3. Sample analysis

Size-fractionated chl-a was measured using a fluorometer

(Trilogy™ fluorometer; Turner Designs, Sunnyvale, CA, USA) after samples were added with 90% acetone and extracted at $-80°C$ for 24 h. Small plankton including picoplankton < 10 μm and nanoplankton $10−20$ μm, and microplankton > 20 μm were analyzed. With targeting phytoplankton < 20 μm, size-fractionated phytoplankton communities were quantified using a flow cytometer (BD AccuriC6™ Becton, Dickinson and Company Franklin Lakes, NJ, USA) at the National Institute of Fisheries Science (NIFS) in Yeosu, South Korea. Eukaryotes (> 2 μm), picoeukaryotes, phycocyanin-containing cyanobacteria (PC cyanobacteria), phycoerythrin-containing cyanobacteria (PE cyanobacteria), and cryptophytes were identified according to (Kang *et al.* 2015) and Kang and Oh (2021). Particle sizes were calibrated using Sphero fluorescence-calibrated glass beads (2 μm; RFP-20-5; Spherotech, Lake Forrest, IL, USA). Dissolved inorganic nutrients were analyzed in duplicate using a SEAL QuAAtro Auto Analyzer (Seal Analytical Ltd., Southampton, UK) at NIFS (Jones 1984; Parsons *et al.* 1984; Price and Harrison 1987).

4. Data analysis

Euphotic depth (Zp) was calculated according to Cloern (1987) that shows an equation of $Zp = 4.61 Kd^{-1}$, where Kd is light extinction coefficient ($Kd = 1.7 Zs^{-1}$) and Zs is transparency measured with a secchi disk. The transparency-driven euphotic depth has been applied to global coastal waters and to Korean coastal waters like Gwangyang Bay

(Lee *et al.* 2017; Kang *et al.* 2020). The 'seacarb' package in a R version 3.6.3 (R Foundation for Statistical Computing, Vienna, Austria) was used to calculate density of three water masses, and a Kruskal-Wallis test with Dunn's test was performed to compare the density of the water masses. To determine the most influential environmental variables to this ecosystem, 'bio-env' analysis was performed, and then using the results, the effects of the variables on the distribution of major phytoplankton groups were assessed through the redundancy analysis (RDA). Correlation analysis (CA) was conducted to exhibit the correlation strength between the important variables and size-fractionated phytoplankton groups. *t*-test was performed to compare the difference in environmental variables between the surface and bottom layers. Statistics were performed using R with packages including 'vegan' for bioenv and RDA (Oksanen *et al.* 2013) and 'corrplot' for CA (Wei *et al.* 2017). Plots were generated using a R package of 'ggplot2' (Wickham 2016) or Ocean Data View (Schlitzer 2015).

RESULTS

1. Spatial distribution of environmental variables

Three water masses were identified as the inner bay,

outer bay, and Yeosu Harbor, and the surface and bottom layers were distinct (Table S1). Surface water temperature ranged from 19 to 21.2°C (mean 20.3°C, Fig. 2A) and bottom water temperature ranged from 16.4 to 18.5°C (mean 17.8°C; Fig. 2F). The lowest temperature on the surface water was at St. 1 (19°C), and water temperature was higher in the inner bay (Fig. 2A). Bottom water temperature distributed similar to the surface water temperature but lowered by mean 2.4°C (Fig. 2F; $p < 0.05$; *t*-test). Mean surface salinity was 34.6 psu with a range of 34.0−35.6 psu (Fig. 2B) and mean bottom salinity was 33.2 psu with a range of 32.9−33.5 psu (Fig. 2G). Surface salinity was highest in the outer bay and lowest near Yeosu harbor (Fig. 2B) while bottom salinity had no discernible difference among stations (Fig. 2G). The salinity difference between the surface and bottom layers was significant ($p < 0.05$; *t*-test). DO ranged 6.8−7.4 mg L^{-1} (mean 7.1 mg L^{-1}) in the surface layer (Fig. 2C) and 7.3−8.3 mg L^{-1} (mean 7.9 mg L^{-1}) in the bottom layer (Fig. 2H). The spatial difference in DO levels was higher in the bottom layer than in the surface layer ($p < 0.05$; *t*-test). In the surface layer, DO concentration was highest in the inner bay (7.4 mg L^{-1}) and decreased toward Yeosu harbor (6.8 mg L^{-1}) and the outer bay (7.0 mg L^{-1}, Fig. 2C). However, in the bottom layer, the outer bay had high DO concentration (8.3 mg L^{-1}, Fig. 2H). The pH in the range of 8.10 to 8.19 showed an average of 8.17 and
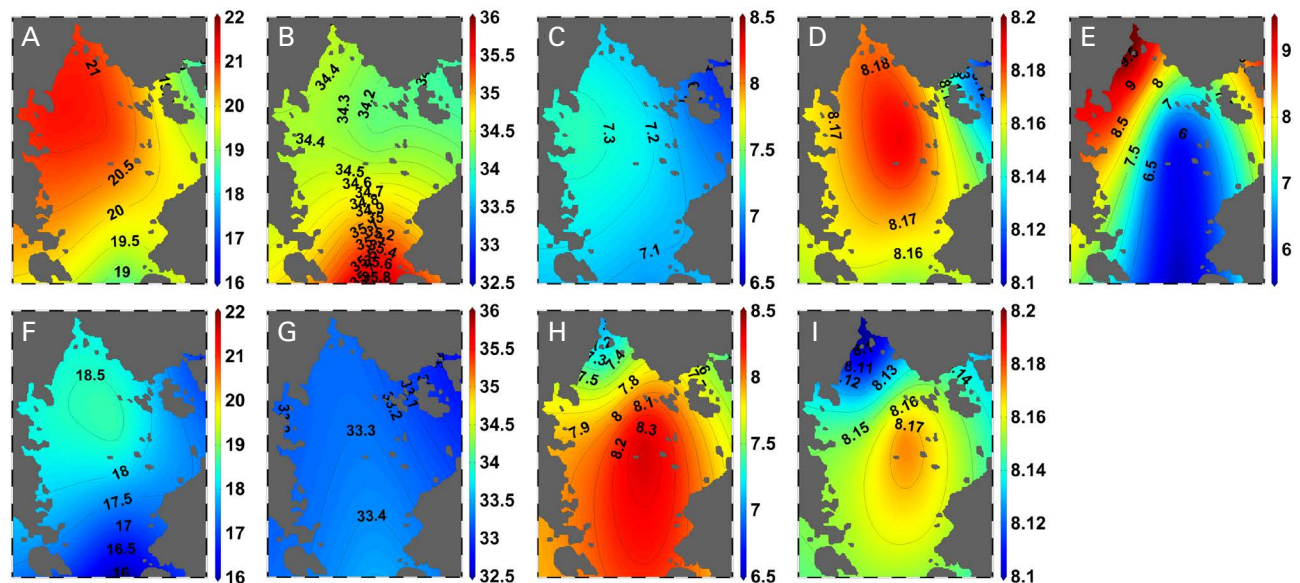

Fig. 2. Physical variables of the surface and bottom waters of Gamak Bay in May 2021. (A) temperature (°C) of the surface water, (B) salinity of the surface water, (C) dissolved oxygen (DO) (mg L^{-1}) of the surface water, (D) pH of the surface water, (E) photic depth (m), (F) temperature (°C) of the bottom water, (G) salinity of the bottom water, (H) DO (mg L^{-1}) of the bottom water, and (I) pH of the bottom water.

8.14 in the surface layer and the bottom layer, respectively. The pH was relatively stable compared to other environmental variables ($p > 0.05$; t-test). The pH was high in the inner bay (8.19) and declined toward the outer bay (8.16) and Yeosu harbor (8.13; Fig. 2D) in the surface layer while it was high in the outer bay (8.17) and low in the inner bay in the bottom layer (8.11; Fig. 2I). Euphotic depth varied from 5.6 to 9.2 m (mean 7.5 m) being the lowest in the outer bay (5.6 m) and deepening toward land (Fig. 2E).

2. Spatial distribution of dissolved inorganic nutrients

NO_3^- levels varied from 0.53−3.24 µm (mean 1.62 µm) in the surface layer (Fig. 3A) and from 0.20−2.66 µm (mean 1.35 µm) in the bottom layer (Fig. 3E). NO_3^- levels were relatively high near Yeosu harbor with 3.24 µm in the surface layer and 2.56 µm in the bottom layer and the outer bay with 2.61 µm in the surface layer and 2.66 µm in the bottom layer (Fig. 3A, E). While NH_4^+ levels were similar between the surface layer (mean 1.50 µm) and the bottom layer (mean 1.49 µm) with a range from 0.52 to 3.28 µm and from 0.64 to 3.06 µm, respectively (Fig. 3B, F), spatially the levels were high near Yeosu harbor (3.38 µm) relative to other region (Fig. 3B, F). PO_4^{3-} levels varied from 0.11−0.32 µm (mean 0.21 µm) in the surface layer (Fig. 3C) and

from 0.11 to 0.36 µm (mean 0.23 µm) in the bottom layer (Fig. 3G) exhibiting the similar levels between two layers and being higher near Yeosu harbor (0.32 µm) and the outer bay (0.31 µm; Fig. 3C, G). $Si(OH)_4$ levels ranged from 10.66 to 13.77 µm (mean 12.10 µm) in the surface layer (Fig. 3D) and from 10.60 to 14.49 µm (mean 12.32 µm) in the bottom layer (Fig. 3H) with the opposite pattern that the highest level was detected in the outer bay in the surface layer (13.77 µm; Fig. 3D) but in the inner bay in the bottom layer (13.39 µm; Fig. 3H). The concentration of dissolved inorganic nutrients was not significantly different between the surface and bottom layers ($p > 0.05$ for NO_3^-, NH_4^+, PO_4^-, $Si(OH)_4$; t-test).

3. Spatial distribution of phytoplankton biomass and community

Total phytoplankton biomass (chlorophyll-a) varied from 1.88 µg L^{-1} in the outer bay to 3.66 µg L^{-1} in the inner bay in the surface layer, whereas each size-fractionated phytoplankton biomass appeared the different spatial distributions (Fig. S1). The microplankton biomass ranged from 1.42 µg L^{-1} in the outer bay to 1.85 µg L^{-1} in the inner bay in the surface layer (Fig. S1B) while the nanoplankton biomass was high in the Yeosu harbor (1.04 µg L^{-1}) and declined toward the outer bay (0.6 µg L^{-1}) and the inner bay
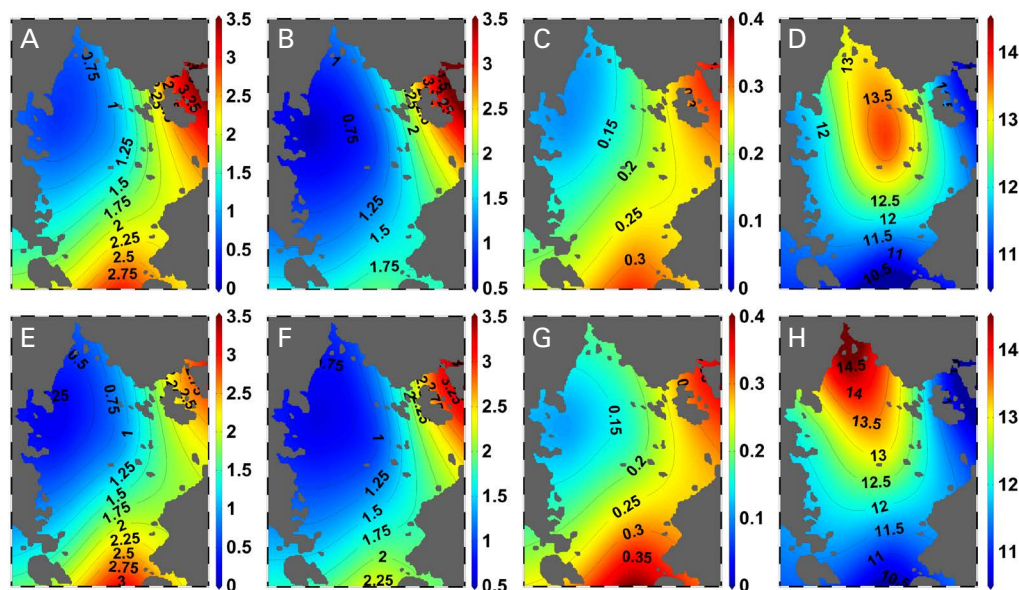

Fig. 3. Spatial variation in dissolved inorganic nutrients in the surface and bottom waters of Gamak Bay in May 2021. (A) NO_3^- content (µm) in the surface water, (B) NH_4^+ content (µm) in the surface water, (C) PO_4^{3-} content (µm) in the surface water, (D) $Si(OH)_4$ content (µm) in the surface water, (E) NO_3^- content (µm) in the bottom water, (F) NH_4^+ content (µm) in the bottom water, (G) PO_4^{3-} content (µm) in the bottom water, and (H) $Si(OH)_4$ content (µm) in the bottom water.
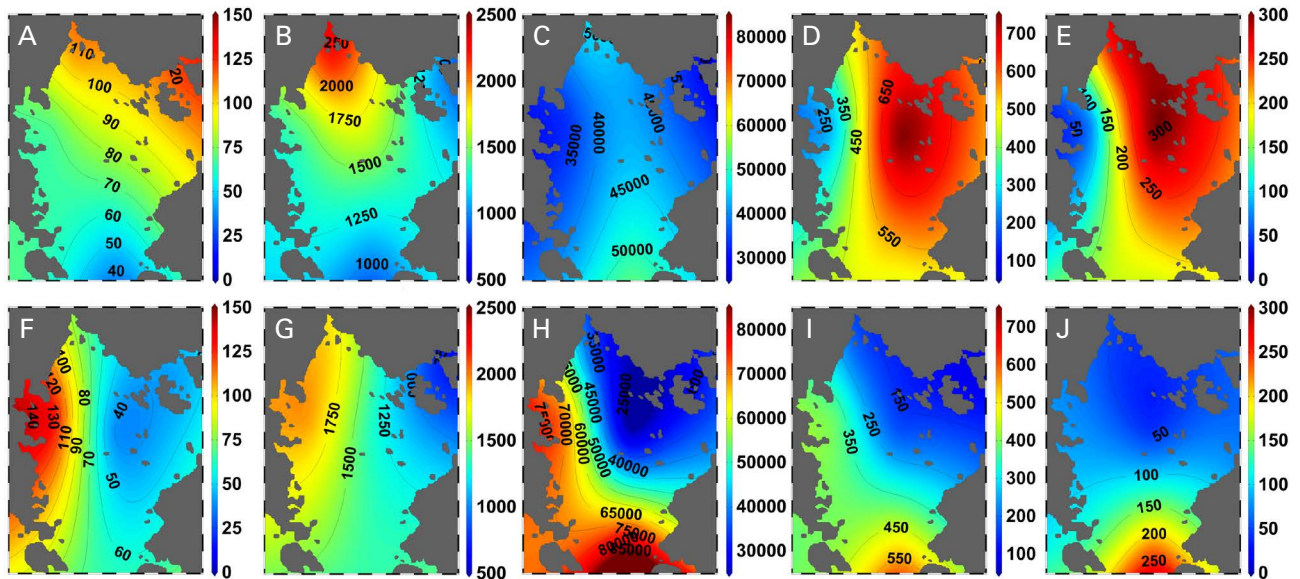
Fig. 4. Spatial distribution of phytoplankton abundance (cells mL^{-1}) quantified by flow cytometry. (A, F) eukaryotes > 2 μm in the surface and bottom waters, (B, G) picoeukaryotes in the surface and bottom waters, (C, H) phycocyanin-containing (PC) cyanobacteria in the surface and bottom waters, (D, I) phycoerythrin-containing (PE) cyanobacteria in the surface and bottom waters, and (E, J) cryptophytes in the surface and bottom waters.

(0.51 μg L^{-1}, Fig. S1C). The picoplankton biomass ranged from 0.74 μg L^{-1} in the Yeosu harbor to 1.34 μg L^{-1} in the inner bay in the surface layer (Fig. S1D).

Phytoplankton communities quantified using a flow cytometer were examined. Abundance of eukaryotes > 2 μm was 45−120 cells mL^{-1} (mean 85 cells mL^{-1}) in the surface layer (Fig. 4A) while that was 40−133 cells mL^{-1} (mean 72 cells mL^{-1}) in the bottom layer (Fig. 4F). In the surface layer, eukaryotes > 2 μm were detected near Yeosu harbor with mean 120 cells mL^{-1} and in the inner bay with mean 67 cells mL^{-1} (Fig. 4A), and the abundance was slightly higher in the bottom layer (mean 133 cells mL^{-1}; Fig. 4F). Picoeukaryote abundance ranged from 1,035 to 2,165 cells mL^{-1} (mean 1,477 cells mL^{-1}) with the highest abundance in the inner bay (mean 2,163 cells mL^{-1}) in the surface layer (Fig. 4B) while the abundance varied from 785 to 1,955 cells mL^{-1} (mean 1,458 cells mL^{-1}) with the highest abundance in the western bay (mean 1,955 cells mL^{-1}) in the bottom layer (Fig. 4G). PC cyanobacteria abundance was much higher in the bottom layer (29,450−84,875 cells mL^{-1}; mean 49,651 cells mL^{-1}; Fig. 4H) than in the surface layer (31,958−50,610 cells mL^{-1}; mean 40,356 cells mL^{-1}; Fig. 4C), and the abundance sharply increased to 84,875 cells mL^{-1} in the outer bay (Fig. 4H). PE cyanobacteria abundance was relatively low compared to PC cyanobacteria abundance with mean 532 cells mL^{-1} in the surface layer

(Fig. 4D) and mean 276 cells mL^{-1} in the bottom layer (Fig. 4I). Cryptophyte abundance was higher in the surface layer (mean 212 cells mL^{-1}; Fig. 4E) than in the bottom layer (mean 90 cells mL^{-1}; Fig. 4J). Abundance of PE cyanobacteria and cryptophytes increased toward Yeosu harbor in the surface layer (Fig. 4D, E) and the outer bay in the bottom layer, whereas the abundance was relatively low in the center of the bay (Fig. 4I, J).

4. Relationship between phytoplankton community and environmental variables

Bio-env analysis using a 'vegan' package on R revealed that salinity, DO, NH$_4^+$, PO$_4^{3-}$, and Si(OH)$_4$ were the most influential factors in the study region (correlation strength = 0.2087; Table 1). Using those environmental variables, RDA was performed to examine the relationship between environmental variables and phytoplankton communities (Fig. 5). The spatial distribution of phytoplankton communities was mainly characterized by salinity, which clearly segregated the surface and bottom layers. While the inner bay communities were mainly correlated with Si(OH)$_4$, the outer bay communities were largely associated with PO$_4^{3-}$ and NH$_4^+$.

Correlation analysis showed that eukaryotes > 2 μm were strongly positively correlated to euphotic depth (cor-

Table 1. Results of 'Bio-env' analysis showing correlations of the most influential variables. Salinity, dissolved oxygen (DO), NH_4^+, PO_4^{3-}, and $Si(OH)_4$ were the variables most significantly correlated to the Gamak Bay ecosystem (correlation of 0.2087)

| Parameter	Size	Correlation
Salinity	1	0.1344
NH_4^+, NO_3^-	2	0.1586
Salinity, DO, NO_3^-	3	0.1838
Salinity, NH_4^+, PO_4^{3-}, $Si(OH)_4$	4	0.1929
Salinity, DO, NH_4^+, PO_4^{3-}, $Si(OH)_4$	5	0.2087
Salinity, Euphotic depth, DO, NH_4^+, PO_4^{3-}, $Si(OH)_4$	6	0.1891
Salinity, Euphotic depth, DO, NH_4^+, NO_3^-, PO_4^{3-}, $Si(OH)_4$	7	0.1863
Temperature, Salinity, Euphotic depth, DO, NH_4^+, NO_3^-, PO_4^{3-}, $Si(OH)_4$	8	0.1468
Temperature, Salinity, Euphotic depth, DO, pH, NH_4^+, NO_3^-, PO_4^{3-}, $Si(OH)_4$	9	0.1277
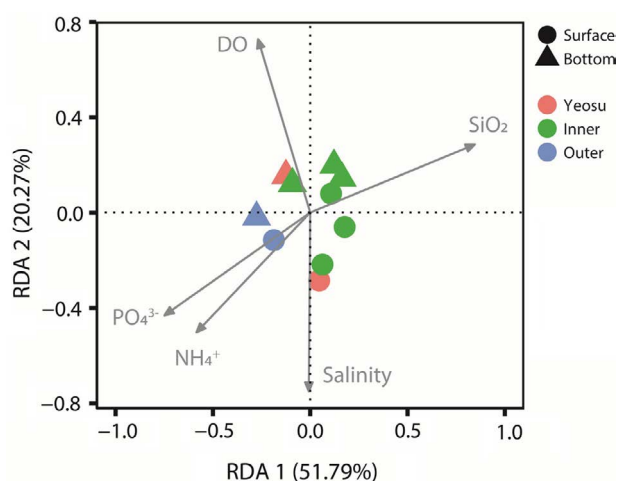
Fig. 5. Redundancy analysis (RDA), presenting the relationship between the major phytoplankton groups and environmental variables in Gamak Bay in May 2021. While the surface and bottom layers were clearly separated by salinity, water masses were characterized by different environmental variables.

Fig. 6. Correlation analysis showing the correlation coefficients between phytoplankton and environmental variables during the study period.

relation coefficient = 0.57; Fig. 6). Picoeukaryotes were positively associated with temperature (0.43) and euphotic depth (0.44) while there were strong negative correlations between picoeukaryotes and dissolved inorganic nutrients ($NH_4^+ = -0.76$, $NO_3^- = -0.81$, and $PO_4^{3-} = -0.80$; Fig. 6). Autotrophic cyanobacteria were related with physical parameters; PC cyanobacteria and PE cyanobacteria were negatively correlated to temperature (-0.40) and DO (-0.42), respectively, but PE cyanobacteria were positively correlated to salinity (0.57; Fig. 6). In the meantime, cryptophytes were positively associated with salinity (0.53), NO_3^- (0.41), and PO_4^{3-} (0.32) but negatively associated with DO (-0.43; Fig. 6).
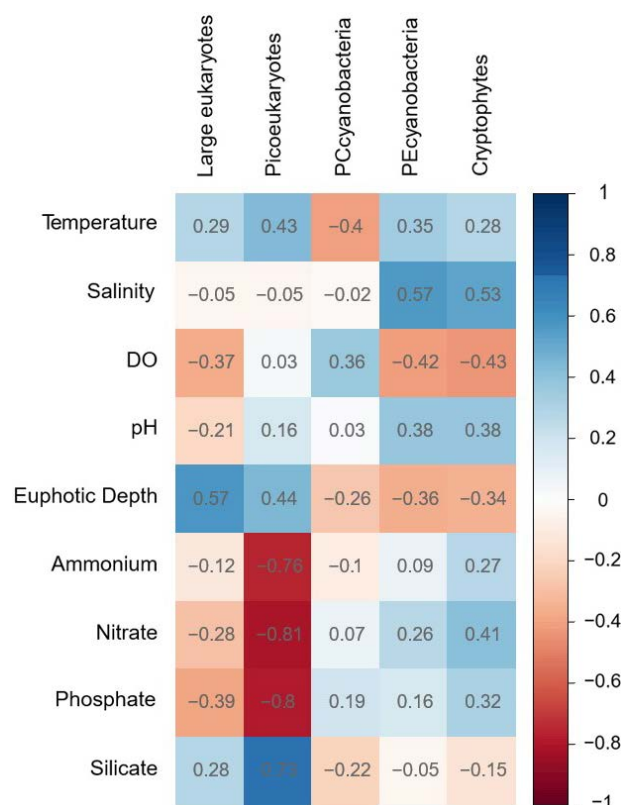
DISCUSSION

1. Environmental characteristics of Gamak Bay in Spring

Water masses were separated into three as the inner bay,

outer bay, and Yeosu Harbor, and the surface and bottom layers were distinct. In particular, the density difference was intensive between the inner bay and outer bay, where freshwater input and offshore seawater input contribute to characterizing the density disparity. Interestingly, bottom salinity was slightly lower than that in the surface waters during the study period. We thoughtfully performed a literature review and searched a source of freshwater, however, unfortunately, we did not find a specific reason for this. In summer, a hypoxic water mass appears in the northern Gamak Bay with low DO and pH (Kim *et al.* 2011). Although pH in the bottom layer of the inner bay was slightly lower than that in the outer bay and the surface layer, DO remained above 2 mg L^{-1}, implying that DO was low but oxygen-deficient water mass was not found (Kim *et al.* 2010).

Light penetration was enhanced in the inner bay and the relatively shallow euphotic depth was confined to the outer bay. Higher light extinction coefficient in the outer bay indicates that the outer bay had higher suspended matter. This is well aligned with the location of the long-lined oyster farms and fish cages shown as the crosshatch pattern and diagonal hatch pattern, respectively, in Fig. 1. Fish farms usually release more organic matter that originate from uneaten food and fecal and urinary products (Bouwman *et al.* 2013b), and tides can translocate the suspended matter in the bay (Lee 2013). Thus, unbroken organic matter from the fish farms moving inward by tides could reduce the euphotic depth in the ecosystem.

Levels of NO$_3^-$, NH$_4^+$, and PO$_4^{3-}$ were high in the outer bay and Yeosu Harbor, whereas Si(OH)$_4$ levels were high in the inner bay. Gamak Bay experiences freshwater input from Yeondeung Creek and Seomjin River (Lee 1992) and outflow from a sewage treatment plant loads to the northern inner bay (Oh *et al.* 2008b). This indicates that high levels of nutrients in the bay originating from river discharge and sewage treatment plant can synergistically affect the phytoplankton growth and biomass in this ecosystem, in addition with the aquaculture farms in the outer bay. Oh *et al.* (2009) illustrated that diatoms were the most dominant phytoplankton group in Gamak Bay due to high levels of Si(OH)$_4$. Because phytoplankton communities were not quantified using a light microcopy or HPLC in this study, we do not firmly conclude the contribution of diatoms to the major phytoplankton groups. However, we suggest that the importance of small phytoplankton should be considered and small phytoplankton were responsible for relatively high composition of phytoplankton communities in Gamak Bay.

2. The spatial distribution of small phytoplankton in Gamak Bay

Regenerated nutrients from uneaten food and urinary production of the aquaculture farms (i.e., fish farms) might enable phytoplankton to access to the available nutrients. Particularly, phytoplankton whose growth is favored by the reduced forms of nutrients (e.g., NH$_4^+$ and Urea) can potentially dominate in an ecosystem (Gobler *et al.* 2013; Kang *et al.* 2021; Kang and Kang 2022). In addition, the role of NH$_4^+$ increases as nutrients originating from sewage treatment plants take a large portion of bioavailable nutrients (Kang *et al.* 2020). The nutrients from the outer bay likely affected the spatial distribution of PC cyanobacteria while nutrients from Yeosu Harbor likely governed the distribution of PE cyanobacteria. In a coastal ecosystem, PC cyanobacteria can exist at a background level even when other picoplankton are dominant and then the picoplankton blooms can succeed to PC cyanobacteria blooms (Kang *et al.* 2015). Likewise, the Gamak Bay ecosystem has a potential for the cyanobacteria proliferation. While picoprokaryotes were positively correlated with nutrients as described above, picoeukaryotes were negatively correlated with most dissolved inorganic nutrients but Si(OH)$_4$. Given that the pico-sized diatoms are detected in the ocean (Rii *et al.* 2018), and that another silicate-dependent picoeukaryote, Bolidophyceae, is widespread from tropics to the pole (Kuwata *et al.* 2018), Si(OH)$_4$ could control the distribution of picoeukaryotes in Gamak Bay.

Nanoplankton, cryptophytes mainly contributed to phytoplankton community in the surface layer of Yeosu Harbor and in the bottom layer of the outer bay and were negatively correlated with euphotic depth. Cryptophytes can endure the low light intensity in turbid waters, where other phytoplankton are not usually able to obtain optimal growth (Barone and Naselli-Flores 2003), and the cryptophyte abundance is often reduced with water quality improvement (Kang *et al.* 2021). The cryptophyte dominance was concomitant with the PE cyanobacteria dominance in the outer bay and Yeosu Harbor, indicating the potential ability of cryptophytes for the mixotrophic nutrient acquisition by consuming PE cyanobacteria (Roberts and Laybourn-Parry 1999; Yoo *et al.* 2017). PC and PE cyanobacteria abundance decreased with the euphotic depth increase, whereas large eukaryote abundance increased with the euphotic depth increase. PC and PE cyanobacteria can exist under a light-deficient condition, in which the water transparency is less than 0.3 m (Gobler *et al.* 2013). Likewise,
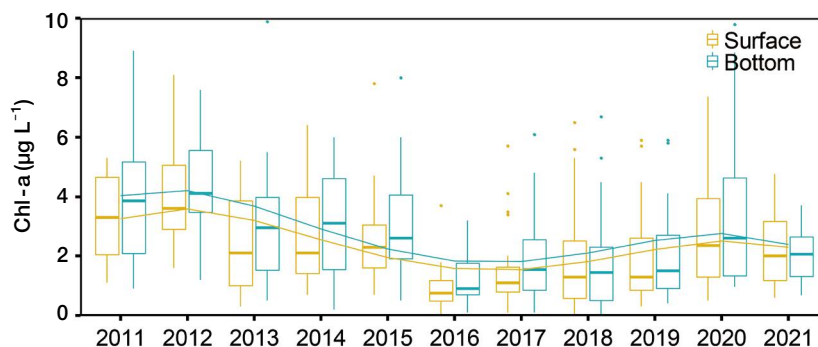
Fig. 7. Long-term variation in chlorophyll-a (chl-a) in Gamak Bay from 2011 to 2021. Chl-a concentrations have declined gradually and remained relatively stable since 2016. The lines are the results from generalized additive models showing the long-term variations in surface and bottom chl-a concentrations.

the high turbidity resulting from aquaculture farm activities might not favor the growth of large eukaryotes but picoeukaryotes did overcome the limitation and dominate the ecological niche.

Despite that Gamak Bay has less salinity gradient than that in the estuarine-coastal continuum like the Seomjin River to Gwangyang Bay region (Bibi *et al.* 2020), salinity also played a major role in defining the spatial distribution of cyanobacteria in Gamak Bay. Cyanobacteria have fairly high resistance to salinity and can adapt to hypersaline environments (Blumwald and Tel-Or 1982; Vonshak *et al.* 1988). In the Gwangyang Bay waters, which are adjacent to our study region, the enhanced ecological role of diverse *Synechococcus* is expected (Kim *et al.* 2018), and PE cyanobacteria, which are typically confined to high salinity waters, can potentially expand their distribution within Gwangyang Bay (Xia *et al.* 2020). Thus, the potential adaptation to a wide range of salinity might enable PC and PE cyanobacteria to be widespread in Gamak Bay. It is necessary to examine the ecological role of PC and PE cyanobacteria in Gamak Bay, particularly related to food consumption in shellfish of the Gamak Bay aquaculture farms.

Long-term trends of chl-a in Gamak Bay had gradually declined until 2016 and in recent years, the chl-a level has remained low (Fig. 7). Because the role of small phytoplankton has been neglected in the coastal phytoplankton studies in South Korea, and the spatial and temporal distribution of diatoms and dinoflagellates were mainly examined in the study region (Oh *et al.* 2008a; Oh *et al.* 2009), which phytoplankton group or size was a principle player for the biomass declining is uncertain. Gamak Bay is responsible for 30% of domestic oyster production in South

Korea (Kim *et al.* 2009) but a water temperature increase and reduction in nutrients led to exacerbating habitats and mass mortality of Pacific oysters (Kim *et al.* 2013). Coastal warming has been more problematic than open ocean because the shallow depth enables coastal waters to experience a rapid warming (Min and Kim 2006), and a shift to small phytoplankton with coastal warming is on-going (Kang *et al.* 2019; Šolić *et al.* 2020). Recently, the oyster production from Gamak Bay was significantly reduced due to the low growth of Pacific oysters (personal communication). Given the dominance of picoplankton or nanoplankton in the bay, the reduction in oyster production of Gamak Bay was likely related to diminishing food supply to oysters. Coastal warming and food supply to shellfish in aquaculture farm have not been intensively examined in the study region. Although picoplankton is relatively important in oligotrophic open oceans (Raven 1998) and our data only present the spring data, picoplankton existed throughout the year and acted a critical role to control the trophic interactions in Gwangyang Bay, adjacent to Gamak Bay (Kang and Oh 2021). Our data also showed the potential role of small phytoplankton as they were abundant in the bay. Therefore, our study stimulates an investigation on the role of size-fractionated phytoplankton in the food webs and fisheries in Gamak Bay, and particularly, we urge that picoplankton should be considered in a coastal water monitoring.

CRediT authorship contribution statement

Yeongji Oh: Investigation, Data curation, Writing-Original draft. Yoonja Kang: Writing-Review & Editing, Supervision, Project administration, Funding acquisition.

ACKNOWLEDGEMENTS

REFERENCES

Agawin NS, CM Duarte and S Agustí. 2000. Nutrient and temperature control of the contribution of picoplankton to phytoplankton biomass and production. Limnol. Oceanogr. 45:591–600. https://doi.org/10.4319/lo.2000.45.8.1891a

Ansotegui A, A Sarobe, JM Trigueros, I Urrutxurtu and E Orive. 2003. Size distribution of algal pigments and phytoplankton assemblages in a coastal-estuarine environment: contribution of small eukaryotic algae. J. Plankton Res. 25:341–355. https://doi.org/10.1093/plankt/25.4.341

Barone R and L Naselli-Flores. 2003. Distribution and seasonal dynamics of Cryptomonads in Sicilian water bodies. Hydrobiology 502:325–329. https://doi.org/10.1023/b:hydr.0000004290.22289.c2

Bibi R, HY Kang, D Kim, J Jang, GK Kundu, YK Kim and CK Kang. 2020. Dominance of autochthonous phytoplankton-derived particulate organic matter in a low-turbidity temperate estuarine embayment, Gwangyang Bay, Korea. Front. Mar. Sci. 7:580260. https://doi.org/10.3389/fmars.2020.580260

Blumwald E and E Tel-Or. 1982. Osmoregulation and cell composition in salt-adaptation of Nostoc muscorum. Arch. Microbiol. 132:168–172. https://doi.org/10.1007/bf00508725

Bouwman AF, A Beusen, C Overbeek, D Bureau, M Pawlowski and P Glibert. 2013a. Hindcasts and future projections of global inland and coastal nitrogen and phosphorus loads due to finfish aquaculture. Rev. Fish. Sci. 21:112–156. https://doi.org/10.1080/10641262.2013.790340

Bouwman L, A Beusen, PM Glibert, C Overbeek, M Pawlowski, J Herrera, S Mulsow, R Yu and M Zhou. 2013b. Mariculture: significant and expanding cause of coastal nutrient enrichment. Environ. Res. Lett. 8:044026. https://doi.org/10.1088/1748-9326/8/4/044026

Cloern JE. 1987. Turbidity as a control on phytoplankton biomass and productivity in estuaries. Cont. Shelf. Res. 7:1367–1381. https://doi.org/10.1016/0278-4343(87)90042-2

Cloern JE. 2018. Why large cells dominate estuarine phytoplankton. Limnol. Oceanogr. 63:S392–S409. https://doi.org/10.1002/lno.10749

Cloern JE, S Foster and A Kleckner. 2014. Phytoplankton primary production in the world's estuarine-coastal ecosystems. Biogeosciences 11:2477–2501. https://doi.org/10.5194/bg-11-2477-2014

Glibert PM, A Al-Azri, J Icarus Allen, AF Bouwman, AH Beusen, MA Burford, PJ Harrison and M Zhou. 2018. Key questions and recent research advances on harmful algal blooms in relation to nutrients and eutrophication. pp. 229–259. In: Global Ecology and Oceanography of Harmful Algal Blooms (Glibert PM, E Berdalet, MA Burford, GC Pitcher and M Zhou, eds.). Springer International Publishing AG. Cham, Switzerland. https://doi.org/10.1007/978-3-319-70069-4_12

Gobler CJ, F Koch, Y Kang, DL Berry, YZ Tang, M Lasi, L Walters, L Hall and JD Miller. 2013. Expansion of harmful brown tides caused by the pelagophyte, *Aureoumbra lagunensis* DeYoe et Stockwell, to the US east coast. Harmful Algae 27:29–41. https://doi.org/10.1016/j.hal.2013.04.004

Jones MN. 1984. Nitrate reduction by shaking with cadmium: alternative to cadmium columns. Water Res. 18:643–646. https://doi.org/10.1016/0043-1354(84)90215-x

Kang Y and CK Kang. 2022. Reduced forms of nitrogen control the spatial distribution of phytoplankton communities: The functional winner, dinoflagellates in an anthropogenically polluted estuary. Mar. Pollut. Bull. 177:113528. https://doi.org/10.1016/j.marpolbul.2022.113528

Kang Y and Y Oh. 2021. Different roles of top-down and bottom-up processes in the distribution of size-fractionated phytoplankton in Gwangyang Bay. Water 13:1682. https://doi.org/10.3390/w13121682

Kang Y, CH Moon, HJ Kim, YH Yoon and CK Kang. 2021. Water quality improvement shifts the dominant phytoplankton group from cryptophytes to diatoms in a coastal ecosystem. Front. Mar. Sci. 8:710891. https://doi.org/10.3389/fmars.2021.710891

Kang Y, F Koch and CJ Gobler. 2015. The interactive roles of nutrient loading and zooplankton grazing in facilitating the expansion of harmful algal blooms caused by the pelagophyte, *Aureoumbra lagunensis*, to the Indian River Lagoon, FL, USA. Harmful Algae 49:162–173. https://doi.org/10.1016/j.hal.2015.09.005

Kang Y, HY Kang, D Kim, YJ Lee, TI Kim and CK Kang. 2019. Temperature-dependent bifurcated seasonal shift of phytoplankton community composition in the coastal water off

southwestern Korea. Ocean Sci. J. 54:467–486. https://doi.org/10.1007/s12601-019-0025-7

Kang Y, YH Kang, JK Kim, HY Kang and CK Kang. 2020. Year-to-year variation in phytoplankton biomass in an anthropogenically polluted and complex estuary: A novel paradigm for river discharge influence. Mar. Pollut. Bull. 161:111756. https://doi.org/10.1016/j.marpolbul.2020.111756

Kim BK, MO Lee and SJ Park. 2012. Characteristics of water temperature and salinity variations, and seawater exchange in Gamak Bay. J. Korean Soc. Mar. Environ. Energy 15:101–110. https://doi.org/10.7846/JKOSMEE.2012.15.2.101

Kim CW, EO Kim, HD Jeong, CG Jung, MW Park and SG Son. 2009. Variation of body composition and survival rate according to spawning of Pacific oyster (*Crassostrea gigas*) in Gamak Bay. Korean J. Fish. Aquat. Sci. 42:481–486. https://doi.org/10.5657/kfas.2009.42.5.481

Kim CW, HJ Oh and YK Shin. 2013. Effects of water temperature on the mass mortality of Pacific oyster, *Crassostrea gigas* in Gamak Bay. Korean J. Malacol. 29:245–250. https://doi.org/10.9710/kjm.2013.29.3.245

Kim JB, SY Lee, J Yu, YH Choi, CS Jung and PY Lee. 2006. The characteristics of oxygen deficient water mass in Gamak Bay. J. Korean Soc. Mar. Environ. Energy 9:216–224.

Kim JB, JI Park, CG Jung, WJ Choi, WC Lee and YH Lee. 2010. Physicochemical characteristics of seawater in Gamak Bay for a period of hypoxic water mass disappearance. J. Korean Soc. Mar. Environ. Saf. 16:241–248.

Kim SY, SH Jun, YS Lee, YH Lee and BM Kim. 2011. Characteristics of phosphate flux at the sediment-water interface in Gamak Bay during the hypoxic water mass. J. Environ. Sci. Int. 20:1069–1078. https://doi.org/10.5322/JES.2011.20.9.1069

Kim Y, J Jeon, MS Kwak, GH Kim, I Koh and M Rho. 2018. Photosynthetic functions of Synechococcus in the ocean microbiomes of diverse salinity and seasons. PLoS One 13:e0190266. https://doi.org/10.1371/journal.pone.0190266

Kim Y, JH Lee, JJ Kang, JH Lee, HW Lee, CK Kang and SH Lee. 2019. River discharge effects on the contribution of small-sized phytoplankton to the total biochemical composition of POM in the Gwangyang Bay, Korea. Estuar. Coast. Shelf Sci. 226:106293. https://doi.org/10.1016/j.ecss.2019.106293

Kuwata A, K Yamada, M Ichinomiya, S Yoshikawa, M Tragin, D Vaulot and A Lopes dos Santos. 2018. Bolidophyceae, a sister picoplanktonic group of diatoms - a review. Front. Mar. Sci. 5:370. https://doi.org/10.3389/fmars.2018.00370

Kwon HK, SJ Oh and HS Yang. 2011. Ecological significance of alkaline phosphatase activity and phosphatase-hydrolyzed phosphorus in the northern part of Gamak Bay, Korea. Mar. Pollut. Bull. 62:2476–2482. https://doi.org/10.1016/j.marpolbul.2011.07.027

Lee GH. 1992. The pattern of sea water circulation in Kamak Bay. Bull. Korean Soc. Fish. Technol. 28:117–131.

Lee JH, D Lee, JJ Kang, HT Joo, JH Lee, HW Lee, SH Ahn, CK Kang and SH Lee. 2017. The effects of different environmental factors on the biochemical composition of particulate organic matter in Gwangyang Bay, South Korea. Biogeosciences 14:1903–1917. https://doi.org/10.5194/bg-14-1903-2017

Lee KH. 2013. Fisheries and oceanography in Gamak Bay. pp. 9–13. In: Proceedings of the Fall Conference of the Korean Society for Marine Environment and Energy. Chonnam National University. Yeosu, Korea.

Lee KH and KD Cho. 1990. Distributions of the temperature and salinity in Kamak Bay. Korean J. Fish. Aquat. Sci. 23:25–39.

Lee MO, JK Kim and BK Kim. 2020. Past, present, and future for the study of Gamak Bay, Korea. J. Korean Soc. Mar. Environ. Energy 23:148–164. https://doi.org/10.7846/JKOSMEE.2020.23.3.148

Min HS and CH Kim. 2006. Interannual variability and long-term trend of coastal sea surface temperature in Korea. Ocean Polar Res. 28:415–423. https://doi.org/10.4217/opr.2006.28.4.415

Oh HT, DJ Kim, WC Lee, RH Jung, SJ Hong, YS Kang, YW Lee and C Tilburg. 2008a. Composition of phytoplankton in Gamak Bay by CHEMTAX Analyses. J. Environ. Sci. Int. 17:1155–1167. https://doi.org/10.5322/JES.2008.17.10.1155

Oh HT, SM Lee, WC Lee, RH Jung, SJ Hong, NK Kim and C Tilburg. 2008b. Sustainability evaluation for shellfish production in Gamak Bay based on the systems ecology 2. environmental accounting for the improvement of the natural environment based on the EMERGY evaluation. J. Environ. Sci. Int. 17:857–869. https://doi.org/10.5322/JES.2008.17.8.857

Oh SJ, JS Park, YH Yoon and HS Yang. 2009. Variation analysis of phytoplankton communities in northern Gamak Bay, Korea. J. Korean Soc. Mar. Environ. Saf. 15:329–338.

Oksanen J, FG Blanchet, R Kindt, P Legendre, PR Minchin, R O'hara, GL Simpson, P Solymos, MHH Stevens and H Wagner. 2013. Package 'vegan'. Community ecology package, version. 2:1–295.

Paerl HW, NS Hall, BL Peierls and KL Rossignol. 2014. Evolving paradigms and challenges in estuarine and coastal eutrophication dynamics in a culturally and climatically stressed world. Estuaries Coasts 37:243–258. https://doi.org/10.1007/s12237-014-9773-x

Parsons TR, Y Maita and C Lalli. 1984. A Manual of Chemical and Biological Methods for Seawater Analysis. Pergamon Press. Oxford, UK. pp. 1–173.

Poulton NJ and JL Martin. 2010. Imaging flow cytometry for quantitative phytoplankton analysis - FlowCAM. pp. 47–54. In: Microscopic and Molecular Methods for Quantitative Phytoplankton Analysis. Intergovernmental Oceanographic Com-

mission, UNESCO. Paris.

Price N and P Harrison. 1987. Comparison of methods for the analysis of dissolved urea in seawater. Mar. Biol. 94:307–317. https://doi.org/10.1007/bf00392945

Raven J. 1998. The twelfth Tansley Lecture. Small is beautiful: the picophytoplankton. Funct. Ecol. 12:503–513. https://doi.org/10.1046/j.1365-2435.1998.00233.x

Rii YM, RR Bidigare and MJ Church. 2018. Differential responses of eukaryotic phytoplankton to nitrogenous nutrients in the North Pacific Subtropical Gyre. Front. Mar. Sci. 5:92. https://doi.org/10.3389/fmars.2018.00092

Roberts EC and J Laybourn-Parry. 1999. Mixotrophic crypto-phytes and their predators in the Dry Valley lakes of Antarctica. Freshw. Biol. 41:737–746. https://doi.org/10.1046/j.1365-2427.1999.00401.x

Schlitzer R. 2015. Ocean data view.

Sinha E, A Michalak and V Balaji. 2017. Eutrophication will increase during the 21st century as a result of precipitation changes. Science 357:405–408. https://doi.org/10.1126/science.aan2409

Šolić M, D Šantić, S Šestanović, N Bojanić, S Jozić, M Ordulj, A Vrdoljak Tomaš and G Kušpilić. 2020. Changes in the trophic pathways within the microbial food web in the global warming scenario: an experimental study in the Adriatic Sea. Microorganisms 8:510. https://doi.org/10.3390/microorganisms8040510

Vonshak A, R Guy and M Guy. 1988. The response of the filamentous cyanobacterium Spirulina platensis to salt stress. Arch.

Microbiol. 150:417–420. https://doi.org/10.1007/bf00422279

Wei T, V Simko, M Levy, Y Xie, Y Jin and J Zemla. 2017. Package 'corrplot'. Statistician 56:e24.

Wickham H. 2016. Package 'ggplot2': Elegant Graphics for Data Analysis. Version 3.2. Springer-Verlag. New York.

Worden AZ, JK Nolan and B Palenik. 2004. Assessing the dynamics and ecology of marine picophytoplankton: the importance of the eukaryotic component. Limnol. Oceanogr. 49:168–179. https://doi.org/10.4319/lo.2004.49.1.0168

Wu W, B Huang and C Zhong. 2014. Photosynthetic picoeukaryote assemblages in the South China Sea from the Pearl River estuary to the SEATS station. Aquat. Microb. Ecol. 71:271–284. https://doi.org/10.3354/ame01681

Xia X, P Lee, S Cheung, Y Lu and H Liu. 2020. Discovery of euryhaline phycoerythrobilin-containing Synechococcus and its mechanisms for adaptation to estuarine environments. mSystems 5:e00842–00820. https://doi.org/10.1128/msystems.00842-20

Yoo DY, KA Seong, HJ Jeong, W Yih, JR Rho, SW Nam and HS Kim. 2017. Mixotrophy in the marine red-tide cryptophyte Teleaulax amphioxeia and ingestion and grazing impact of cryptophytes on natural populations of bacteria in Korean coastal waters. Harmful Algae 68:105–117. https://doi.org/10.1016/j.hal.2017.07.012

Yoon Y. 2000. Variational characteristics of water quality and chlorophyll-a concentration in the northern Kamak Bay, Southern Korea. J. Korean Environ. Sci. Soc. 9:429–436.
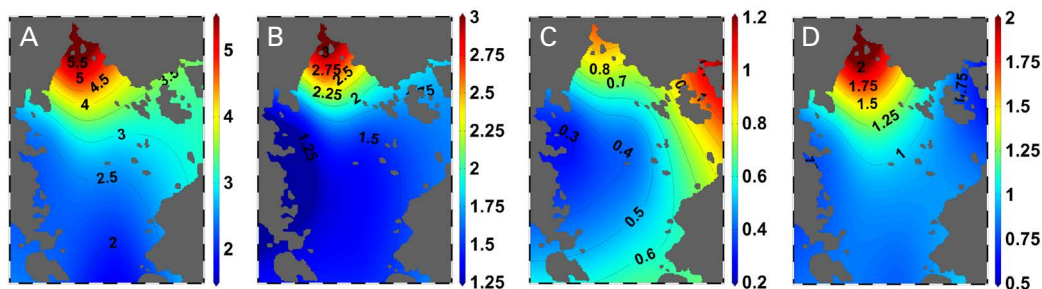
SUPPLEMENTARY MATERIALS

Fig. S1. Spatial distribution of size-fractionated chl-a in the surface waters of Gamak Bay in May 2021. (A) Total chl-a, (B) chl-a of small phytoplankton ($< 10\,\mu m$), (C) chl-a of nanoplankton, and (D) chl-a of microplankton.

Table S1. Density of three water masses and that of surface and bottom waters. The Kruskal-Wallis test was performed with Dunn's test. The density between the surface and bottom waters was significantly different ($p < 0.05$). The density between the inner bay and outer bay was significantly different ($p < 0.05$), whereas the density between the inner bay and Yeosu Harbor ($p > 0.05$) and the density between the outer bay and Yeosu Harbor were not significantly different ($p > 0.05$)

Water mass	Surface waters	Bottom waters
Yeosu	1024.303	1023.857
Inner	1023.982	1023.827
Outer	1025.402	1024.472